HHS Public Access

Author manuscript

Cancer Gene Ther. Author manuscript; available in PMC 2015 March 09.

Published in final edited form as:

Cancer Gene Ther. 2014 June ; 21(6): 228–237. doi:10.1038/cgt.2014.22.

Evaluation of apoptogenic adenovirus type 5 oncolytic vectors in a Syrian hamster head and neck cancer model

S. Vijayalingam[#1], **Mohan Kuppusamy**[#1], **T. Subramanian**[1], **Frank F. Strebeck**[2], **Cheri L. West**[2], **Mark Varvares**[3], and **G. Chinnadurai**[1]

[1]Institute for Molecular Virology Saint Louis University School of Medicine 1100 South Grand Blvd, St. Louis, MO 63104

[2]Department of Comparative Medicine Saint Louis University School of Medicine 1100 South Grand Blvd, St. Louis, MO 63104

[3]Department of Otolaryngology, Head and Neck Surgery Saint Louis University Cancer Center 3655 Vista Ave, West Pavilion, St. Louis, MO 63110

[#] These authors contributed equally to this work.

Abstract

Human adenovirus (HAdV) vectors are intensely investigated for virotherapy of a wide variety of human cancers. Here, we have evaluated the effect of two apoptogenic HAdV5 vectors in an immunocompetent Syrian hamster animal model of head and neck cancer. We established two cell lines of hamster cheek pouch squamous cell carcinomas, induced by treatment with 9, 10-dimethyl-1, 2-benzanthracene (DMBA). These cell lines, when infected with HAdV5 mutants *lp*11w and *lp*11w/Δ55K (which are defective in the expression of either E1B-19K alone or both E1B-19K and E1B-55K proteins) exhibited enhanced apoptotic and cytotoxic responses. The cheek pouch tumor cells transplanted either subcutaneously at the flanks or in the cheek pouches of hamsters readily formed tumors. Intra-tumoral administration of HAdV5 E1B mutants efficiently suppressed the growth of tumors at both sites. Histological examination of orthotopic tumors revealed reduced vascularity and the expression of the viral fiber antigen in virus-administered cheek pouch tumors. These tumors also exhibited increased caspase-3 levels, suggesting virus-induced apoptosis may contribute to tumor growth suppression. Our results suggest that the apoptogenic HAdV5 vectors may have utility for the treatment of human head and neck cancers.

Keywords

adenovirus; apoptosis; Syrian hamster; cheek pouch; head and neck cancer

Correspondence G. Chinnadurai, Chinnag@slu.edu or Mark Varvares, varvares@slu.edu.

Conflict of Interest: The authors do not have any conflict of interest.

Introduction

The incidence of head and neck cancers is rapidly increasing and these cancers result in more than 12,000 deaths annually in the US. Additionally, about 500,000 new cases of these cancers are diagnosed every year globally [1]. Head and neck cancers are predominantly of squamous cell carcinoma (HNSCC) histology and constitute the sixth most prevalent cancer worldwide. They are considered 'difficult' cancers since they are relatively more resistant to conventional treatment modalities such as chemotherapy and radiotherapy [2-4]. It appears that the resistance of HNSCCs to chemotherapy and radiotherapy may be linked to enhanced expression of anti-apoptosis proteins such as BCL-xL and MCL-1 [5]. The activation of these pro-survival proteins may be linked to the enhanced expression of the epidermal growth factor receptor (EGFR) and EGFR-signaling. Although the treatment of HNSCC with tyrosine kinase inhibitors remains a primary treatment modality at present (reviewed in [6]), other exploratory approaches aimed to enhance the apoptotic death of HNSCC have also been reported. Peptides and BH3 mimetics that bind with the BH3 domain of BCL-2 family pro-survival proteins were shown to enhance the sensitivity of chemotherapeutic drugs in HNSCC [7, 8]. Considering the relative resistance of HNSCC, other alternative therapeutic approaches for the management of this disease is needed. The use of viral vectors that kill cancer cells alone or in combination with other treatment modalities appears to be a promising approach.

We have previously reported that infection of HNSCC cell lines with an apoptogenic HAdV5 mutant (*lp*11w) that is defective in coding for the viral anti- apoptosis protein E1B-19K, resulted in reduced levels of BCL-2 family pro-survival proteins and the infected cells exhibited enhanced apoptotic response [9]. In HNSCC cells infected with *lp*11w, there was dramatic down regulation of EGFR as a result of enhanced proteolysis during virus-induced apoptosis as well as by the direct action of the HAdV5 E3-RID protein complex, which targets membrane-associated receptors for proteolysis. These *in vitro* results suggested the potential utility of *lp*11w as a virotherapeutic agent for HNSCC.

HAdV5 mutants that are defective in a second protein coded by the E1B region, E1B-55K, are wildly used as oncolytic vectors against several cancers in preclinical and clinical studies. The 55K protein is multifunctional and is required for efficient viral replication. It functions through diverse mechanisms [10]. E1B-55K and its cooperating viral protein, E4orf6 form an E3 ligase complex that targets p53 and components of the DNA repair machinery for proteasomal degradation. During late stages of viral infection, it plays a role in selective nucleo-cytoplasmic export of viral mRNAs and has been postulated to be the mechanism governing the oncolytic activity of E1B-55K mutants [11]. The treatment of HNSCC with a replication competent HAdV5 vector, ONYX-015 that is defective in the expression of E1B-55K protein, in combination with chemotherapeutic agents cisplatin and 5-flurouracil resulted in enhanced oncolysis [12]. In addition to E1B-55K deleted vectors, the use of other replication competent and replication defective HAdV vectors for the treatment of advanced head and neck cancers have been explored. Certain conditionally replicating oncolytic adenovirus vectors that selectively replicate in tumor cells have been employed to kill HNSCC in xenografts and tumor explants [13-15]. An HAdV5 replication-defective vector that

expresses the tumor suppressor protein p53 (Adp53) is in advanced clinical trials [16-18] and is an approved agent in China for the treatment of HNSCC (reviewed in [19]).

In the present study, we chose to investigate the anti-tumor activity of HAdV5 mutant *lp*11w as well as a second apoptogenic HAdV5 mutant that is defective in coding for both E1B proteins (*lp*11w/Δ55K) in the Syrian hamster animal model. The rationale for the use of these vectors is to exploit their powerful pro-apoptotic activity to kill the tumor cells. Although most of the preclinical studies on the use of HAdV5 vectors employed immunodeficient nude mouse bearing human tumor xenografts, recent studies have exploited the Syrian hamster as an immunocompetent small animal model (which supports HAdV5 replication) to evaluate the oncolytic activity of HAdV5 vectors [20-22]. In order to evaluate the apoptogenic HAdV5 vectors against head and neck tumors, we developed two Syrian hamster cell lines from the cheek pouch squamous cell carcinoma induced by the chemical carcinogen DMBA and determined the oncolytic activity of the HAdV5 vectors in orthotopic and heterotopic tumors induced by these cell lines. Our study appears to be the first in which HAdV5 vectors have been tested in an orthotopic HNSCC tumor model.

Materials and methods

Cells

The human cell lines A549 (alveolar carcinoma), MCF7 (breast carcinoma), HeLa and IMR90 fibroblasts were obtained from the American Type Culture Collection (ATCC, Bethesda, MD, USA). The human embryonic kidney 293 (HEK-293) cells were from Microbix (Toronto, ON, Canada). The hamster pancreatic carcinoma cell line SHPC6 [23] was obtained from Dr. W.S. M. Wold. Normal human bronchial epithelial (NHBE) cells were obtained and grown in a specific medium from Cambrex (Walkersville, MD, USA). Normal human foreskin fibroblasts (HFF) were gift from Dr. R. Ray. A549, 293 and HFF cells were grown in DMEM (Sigma Life Science, St. Louis, USA) supplemented with 10% FBS.

Establishment of Hamster pouch tumor cell lines

Four to six week-old female Syrian Hamsters were anesthetized using 3% isoflurane; their cheek pouches were painted with 0.5% DMBA (9, 10-dimethyl-1, 2-benzanthracene #D3254,Sigma) in paraffin oil (#18512, Sigma) using camel hair brush No.4 (#6020-04000, Gordon Brush) twice a week for 12 to 14 weeks [24, 25]. The tumors were aseptically harvested from euthanized animals and transferred to RPMI media without serum. The cells from the tumors were prepared using a commercial kit (Cancer cell isolation kit - #C100XX, Panomics, Affymetrix) and plated in DMEM supplemented with 20% FBS, 10 μg/mL of hydrocortisone, 50 ng/mL of epidermal growth factor (EGF), 5 μg/mL of spermine and antibiotics [26]. The cells were further cultured in DMEM supplemented with 10% FBS with antibiotics. DMBA-induced buccal tumor cells (2×10^{7}) were transplanted subcutaneously in the flanks. Ten days after injection the tumors were aseptically removed and the cells were prepared and clonal cell lines (HPT11 and 12) were established.

Subcutaneous tumor assay in nude mice

Hamster cheek pouch SCC tumor (HPT12) cells (4×10^6) were injected subcutaneously in 100 μl volume into 5-6 week-old female athymic nude mice (Harlan Sprague Dawley, Indianapolis, IN, USA) into the hind flanks to establish subcutaneous tumors. Tumor bearing animals were randomized prior to virus injection. When the tumor volumes reached about 100 to 200 μl, the mice were injected intratumorally with 50 μl vehicle (phosphate buffered saline with 1 mM $MgCl_2$ and 1 mM $CaCl_2$ (PBS++) alone or with 1×10^9 PFU of *dl*312 or HAdV5 wt or *lp*11w or *lp*11w/Δ55K for six consecutive days (total 6×10^9 PFU/animal). Tumor sizes were measured twice weekly with a Sylvac digital caliper and the volumes were calculated using the formula length × width^2/2.

Subcutaneous and cheek pouch SCC tumor assays in hamsters

Four to five week-old male Syrian hamsters (Harlan Sprague Dawley Indianapolis, IN) were subcutaneously injected with 1×10^7 hamster cheek pouch SCC tumor cells in 200 μl volume into the hind flanks to establish subcutaneous tumors. In another set of experiments, 1×10^7 hamster SCC tumor cells were injected submucosally in 200 μL volume into the right cheek pouches. Tumor bearing hamsters were randomized and when the tumor volumes reached about 100-200 μl, the animals were intratumorally injected with 100 μl vehicle (PBS++) alone or with 1×10^{10} PFU of *lp*11w or *lp*11w/Δ55K for six consecutive days (total 6×10^{10} PFU/animal). Tumor measurements were performed twice weekly.

Western blot

Cells were grown in 60 mm tissue culture dishes and washed twice with PBS. Cells were lysed in NuPAGE sample buffer and heated in boiling water for 5 min. The extracts were fractionated by SDS–PAGE (NuPAGE 4-12% gel, NOVEX, Life technologies, USA) and subjected to Western blotting. The following antibodies were used: anti-cytokeratin 19 (sc-25724, Santa Cruz), cytokeratin 8 (17514-1-AP, Proteintech), cytokeratin 14 (22221-1-AP, Proteintech), anti-EGFR (sc-03, Santa Cruz), anti-actin (sc-1615, Santa Cruz), caspase-3 (9662, Cell Signaling), PARP (556362, BD Bioscience), E1A (05-595, Millipore), E1B 19K (gift from Dr. M. Green) and E1B-55K (gift from Dr. Peter Yaciuk) Abs.

Viral growth assay

A549, NHBE and HFF cells were plated in 35 mm dishes and at 60 to 70 % confluency, were infected with HAdV5 mutants. A549 and NHBE cells were infected at 10 PFU/cell while HFF cells were infected at 100 PFU/cell. One hr after infection, the cells were washed three times with medium containing no serum and fed with 2.5 ml of DMEM containing 5% fetal calf serum. After forty hours, the cells and the medium were harvested and the viruses were released by freeze, thaw and sonication and the virus yield was estimated by plaque assay on 293 cells.

Determination of virus titer in hamster serum

At the end of the experiments hamsters were sacrificed, blood was collected in sterile tubes without anticoagulant from each animal and allowed to stand for about 10-20 min. The

samples were centrifuged at 1500×g for 10 min and the serum was removed and frozen at −80°C. The serum samples were tittered by plaque assay on 293 cells.

Neutralizing antibody titration

All serum samples were heat inactivated at 56°C for 30 min prior to titration. They were diluted two fold across 96 well plates in four replicates. One column without serum sample and the other column without virus were run as controls. All wells except virus control were incubated with 100 PFU/well of HAdV5 wt. After one hr, 5×10^3 A549 cells in growth medium were added to each well and incubated for 8 to 10 days at 37°C. At the end of the incubation period neutral red (30 fold dilution of neutral red in PBS) was added to the cells and incubated for one hr at 37°C. The plates were gently rinsed with PBS two times followed by the addition of 100 μL acidified ethanol (50% ethanol in 1% acetic acid in water). After 10 min at room temperature, the plates were read at 550 nm using a plate reader and the neutralizing antibody titers were calculated

Histology

Solid tumors were fixed in formalin and 2-3 mm thick slices were excised with a sharp scalpel through the middle of each tumor. The slices were fixed for another 24 hr in formalin, processed into paraffin in a Miles Scientific Tissue-Tek VIP autoprocessor, embedded in cassettes in a Leica EG1150H/1150C embedding station, and sectioned at 5 μm with a Leica RM2255 microtome using disposable steel blades. After collection on Fisher Super Frost glass slides the sections were stained with hematoxylin and eosin in a Leica Autostainer XL and after coverslipping with Leica Surgipath MM24 mounting medium were photographed with an Olympus BX41 microscope/DP72 digital camera system. Contrast and brightness were adjusted using Microsoft Power Point.

Immunohistochemistry

Slides of 5 μm thick formalin-fixed paraffin sections were de-paraffinized and subjected to antigen retrieval using DIVA Decloaker solution (Biocare Medical, Concord, CA). Following quenching of endogenous peroxidase with 3% hydrogen peroxide in PBS for 30 min the sections were washed in PBS and blocked (1% bovine serum albumin, 5% normal goat serum, 0.05% TX100 in PBS) for 30 min at room temperature in a humidified sealed container. Sections were then incubated overnight at 4° C in anti-fiber adenovirus Ab4 monoclonal antibody (4D2; MS-1027-P, NeoMarkers, Freemont, CA) or anti-caspase-3 antibody (9662, Cell Signaling) diluted 1:200 in $1/10^{th}$ blocking buffer in a sealed humidified container. Negative controls were incubated in non-immune isotype-specific mouse IgG (Sigma I5381) at the same IgG protein concentration as for the anti-fiber primary antibody. The sections were then washed in PBS and incubated for 1 hr at room temperature in goat anti-mouse IgG conjugated to peroxidase (Sigma A4416) diluted 1:400 in $1/10^{th}$ blocking buffer. After washing in PBS, the sections were incubated in peroxidase substrate (Sigma D4168) for 5 min and the reaction was stopped by rinsing in water. The sections were counter-stained with hematoxylin, dehydrated, coverslipped with Leica Surgipath MM24 mounting medium and photographed as described above. Histology and immunohistochemistry staining were performed at the Research Microscopy and Histology Core, Saint Louis University School of Medicine.

FACS Analysis

HPT11 and HPT12 cells (4×10^5) were infected with 400 PFU of indicated adenovirus. After 24 hr, infected cells were trypsinized, washed with PBS and binding buffer preceded by Annexin APC and PI staining according to manufacturer instructions (Annexin V Apoptosis Detection Kit APC cat.no. 88-8007, eBioscience). Cells were analyzed using a FACS Calibur flow cytometer (Beckman Dickinson).

Statistical analysis

The data from multiple samples were compared by Student's t-tests analysis, 2-way ANOVA by Bonferroni multiple comparisons. Significant values were defined as those *p* values of ≤0.05.

Results

HAdV5 vectors

We have previously reported that the replication competent apoptogenic mutant of HAdV5, *lp*11w exhibited enhanced cytolytic activity in human HNSCC cells *in vitro* [9]. The apoptogenic activity of *lp*11w is conferred by a mutation that obliterates the ORF for the viral anti-apoptotic protein E1B-19K [27]. In the present study, we also used an additional vector that is defective in coding both E1B-19K and E1B-55K proteins (Fig. 1A). We decided to include the mutation in E1B-55K, since HAdV5 mutants have been reported to exhibit restricted replication in certain normal human cells [28]. We rationalized that this vector, designated here as *lp*11w/Δ55K, would incorporate both the enhanced apoptotic activity in cancer cells and reduced toxicity to normal cells. As expected, the newly engineered mutant (*lp*11w/Δ55K) was deficient in the expression of both E1B proteins while *lp*11w was deficient in the expression of only E1B-19K (Fig. 1B). Additionally, *lp*11w/Δ55K also expressed reduced levels of E1A proteins. We assessed the replication of these vectors in comparison with HAdV5 wt in normal human bronchial epithelial (NHBE) cells and in normal human foreskin fibroblasts (HFF) (Fig 1C). In NHBE, replication of both *lp*11w and *lp*11w/Δ55K was significantly reduced compared to HAdV5 wt. In contrast, the replication of *lp*11w was not impaired in HFF while replication of *lp*11w/Δ55K was severely impaired. These results suggest that the lack of E1B-19K in these vectors may reduce toxicity to normal epithelial cells during oncolytic applications to head and neck cancers. The combination of both E1B-19K and 55K mutations may retard replication in both NHBE and HFF.

Hamster pouch tumor cell lines

The hamster pouch tumor model is a well-accepted orthotopic head and neck cancer [29]. Since HAdV5 replicates in the Syrian hamster, it has been shown to be a valuable immune-competent model to investigate the oncolytic activity of HAdV5 vectors (reviewed in [30]). In order to evaluate the HAdV5-E1B vectors for head and neck cancers, we first explored the utility of the hamster pouch tumors induced by painting with the chemical carcinogen DMBA. However, we encountered difficulty in quantifying the effect of intra-tumoral administration of the viral vectors in this system due to the heterogeneity of large number of

tumors induced by DMBA on the painted area. Therefore, we decided to use syngeneic pouch tumor cell lines that could be transplanted in the pouch for more quantitative evaluation of HAdV5-E1B vectors. We established two clonal cell lines derived from pouch squamous cell carcinomas (hamster pouch tumor, HPT) induced by treatment with DMBA. We examined the expression of the squamous cell carcinoma markers, cytokeratins 8, 14 and 19 [3132, 33] in these cell lines (Fig. 2A). Both cell lines expressed readily detectable levels of all three cytokeratins. To determine whether the viral vectors induce cytolysis of these cell lines, the cells were infected with HAdV5 wt or different mutants and cell lysis was quantified by the lactate dehydrogenase (LDH) release assay (Tollefson, 1996) (Fig. 2B). In both hamster pouch tumor cell lines, mutant *lp*11w induced substantially increased release of LDH compared to HAdV5 wt. The mutant *lp*11w/Δ55K induced intermediate levels of LDH release. These results suggest that both E1B mutants may be more cytotoxic to the hamster pouch tumor cell lines than HAdV5 wt. Between the two E1B mutants, *lp*11w may be a more potent cytolytic agent than *lp*11w/Δ55K.

Apoptotic activity of E1B mutants in hamster cells

It is well known that HAdV mutants deficient in the expression of the viral anti-apoptosis protein E1B-19K induce apoptosis in cultured animal cells [34, 35]. We examined the apoptotic activity of the E1B mutants in the hamster tumor cell lines by analyzing the activation of caspase-3 as well as proteolytic processing of poly ADP-ribose polymerase (PARP) and epidermal growth factor receptor (EGFR). Both E1B mutants induced efficient caspase-3 activation (loss of procaspase 3 and formation of 19 kD and 17 kD subunits) and proteolytic processing of PARP and EGFR (caspase target proteins), suggesting efficient apoptosis induction by *lp*11w and *lp*11w/Δ55K in both HPT11 and 12 cell lines (Fig. 3A). We also measured the levels of apoptosis by FACS analysis of cells stained with annexin V-APC and the non-vital stain propidium iodide (PI). In both cell lines infected with either E1B mutants, there was increased apoptosis as indicated by annexin V-staining and total cell death (PI-staining) (Fig. 3B, C). The cell population in the transition phase (apoptosis to dead, positive for both Annexin V and PI staining) also showed comparable patterns. These results show that both E1B mutants are apoptogenic in the hamster pouch tumor cell lines.

Tumor growth suppression by E1B mutants

We first determined the effect of the viral vectors *lp*11w and *lp*11w/Δ55K in the mouse xenograft model (Fig. 4A). Athymic mice were transplanted with HPT12 cells subcutaneously and the tumors were then treated by intratumoral injection with different HAdV5 mutants. In this tumor model, both *lp*11w and *lp*11w/Δ55K suppressed tumor growth efficiently compared to *dl*312 (replication defective control). Although HAdV5 wt inhibited tumor growth, the effect was less compared to the E1B mutants. We then determined the effect of *lp*11w and *lp*11w/Δ55K in subcutaneous hamster flank tumors induced by the transplantation of the two hamster tumor cell lines. The hamsters bearing HPT12-induced tumors were treated with different HAdV5 mutants by intratumoral injection and the changes in tumor volumes were monitored for three weeks. In tumors injected with mutant *dl*312, there was substantial increase in volumes (Fig. 4B). In contrast, there was no significant increase in tumor volumes in animals injected with *lp*11w or *lp*11w/Δ55K during the period of observation compared to animals injected with *dl*312. The

oncolytic activities of the E1B mutants were also assessed against tumor bearing hamsters that were subcutaneously transplanted in the flanks with the tumor cell line HPT11. In these tumors, both E1B mutants efficiently inhibited tumor growth compared to the administration of vehicle alone (Fig. 4C). These results suggested that the apoptogenic E1B mutants efficiently inhibited tumor growth both in the xenograft and syngeneic models transplanted with the hamster pouch tumor cell lines.

Since the E1B mutants exhibited significant anti-tumor activity against subcutaneous tumors in the flanks of athymic mice and hamsters, we then determined the effect of these mutants against orthotopic tumors in hamster pouches. The hamster pouch tumor cell lines were transplanted submucosally in the Syrian hamster cheek pouches. Both cell lines formed tumors in a more accelerated fashion in the pouches than in the flanks. Since there was no significant difference in tumor growth in the pouch of animals treated with the vehicle or *dl*312 (results not shown), the effects of E1B mutants were compared with the effects of vehicle administration in these tumor assays. Between the two cell lines, HPT12 formed faster growing tumors than HPT11. Intratumoral administration of *lp*11w and *lp*11w/Δ55K inhibited the growth of tumors induced by both cell lines (Fig. 5). We note that in some instances, viral administration induced transient inflammation in the tumors that skewed the measurements at certain time points (*e.g.*, Fig. 5A, 7 days).

Tumor histology

Histological examination of the pouch tumors collected after sacrifice at 17 days from vehicle treated animals revealed clear submucosal localization (Fig. 6A, top panel) and increased angiogenesis and vascular ectasia with thrombosis, while tumors administered with the viruses exhibited reduced vascularity (Fig. 6A, lower panel). The virus-treated tumors also showed large areas of confluent necrosis (Fig. 6B. top panels; indicated by arrow heads) and focal areas of dystrophic calcification (Fig. 6B, lower panels, indicated by arrows) compared to vehicle-administered tumors. Further, the tissues surrounding the virus-administered tumors also contained more cells that resembled aggregates of the plasma cells (Fig. 6C, top panels) and infiltration of mast cells (Fig. 6 C, lower panels, indicated by arrows) than the tissues surrounding the vehicle-administered tumors. The presence of features such as chromatin condensation associated with apoptosis was also prevalent in virus-treated tumors (Fig. 6D).

We then analyzed the pouch tumor samples and the plasma from virus-treated animals at the end of the study for infectious virus by plaque and infectious center assays on sensitive human (293) cells. However, these assays did not reveal the presence of infectious virus at detectable levels (results not shown). We also analyzed the tumor sections by immunocytochemistry to detect the viral fiber antigen (Fig. 7A) and caspase-3 (Fig. 7B). In tumors treated with *lp*11w focal positive staining patterns for fiber at discrete locations were observed (Fig. 7A-3) while in tumors treated *lp*11w/Δ55K (Fig. 7A-4) more extensive staining was noted. These results suggest that the virus-treated tumors may support at least limited late viral gene expression. The virus-treated tumors were also significantly positive for caspase-3 staining, suggesting virus-induced apoptosis.

The sera from tumor bearing hamsters collected at the end of the tumor assays were analyzed for anti-viral antibodies (Table 1). These results revealed the presence of neutralizing antibodies against HAdV5. These results suggest that the treatment of hamsters with the cytolytic viral vectors induced significant antibody response against viral antigens.

Discussion

We have investigated the potential utility of two apoptotically proficient HAdV5 vectors against two head and neck model hamster cell lines in the immunocompetent Syrian hamster model. Most preclinical studies with oncolytic HAdV vectors have employed xenografts of human cancer cell lines in athymic mice. Recently, the Syrian hamster has been exploited as an immunocompetent model that is permissive for HAdV5 replication (reviewed in [30]). A limitation for the use of the hamster system has been the availability of suitable syngeneic tumor cell lines. Here, we established two cell lines from the Syrian hamster cheek pouch squamous cell carcinomas that readily form orthotopic tumors upon submucosal transplantation in the cheek pouches as well as heterotopic tumors at the flanks upon subcutaneous transplantation. Between the two vectors, *lp*11w exhibited enhanced cytolytic activity in the two hamster cell lines than *lp*11w/Δ55K *in vitro* (Fig. 2B). However, both vectors suppressed the growth of orthotopic and heterotopic tumors at comparable levels. Thus, it is possible that the virus-induced apoptotic response might contribute to their oncolytic activity. Extensive analysis of the tumor samples and the plasma from virus-treated hamsters at the end of the study did not provide evidence for the presence infectious virus (results not shown). However, immunocytochemistry analysis of the tumor samples revealed the presence of different levels of the viral fiber antigen (Fig. 7A). Thus, it is possible that there might be low levels of abortive/productive viral replication within the tumors. These tumors also contained hallmarks of apoptosis such as chromatin condensation (Fig. 6D) and activation of caspase-3 (Fig. 7B). Thus, the apoptotic activity of the two vectors may restrict the level of viral replication in the tumors as well as contribute to reduced tumor growth. Considering the lack of detectable levels of infectious virus within the tumors, it is possible that the apoptotic activity of the two vectors might be the driver behind their strong oncolytic activity. It should be noted that other investigators who studied other oncolytic HAdV5 vectors that do not exhibit enhanced apoptosis also failed to detect significant viral replication in virus-treated hamsters at late times after infection [36, 37]. The cytolytic activity of these vectors may also facilitate the release of complete or incomplete virus particles from infected tumor cells contributing to the anti-viral immune response (Table 1) and tumor growth inhibition.

One of the characteristic features of HNSCC is overexpression of EGFR [38, 39] which form the basis for the treatment of these cancers with EGFR antagonists. We have previously shown that in HNSCC cells infected with *lp*11w, there was a dramatic down-regulation of EGFR as a result of caspase-mediated proteolytic processing of EGFR as well as through viral E3-RID protein-mediated receptor clearing [9, 40, 41]. In the hamster tumor cell lines infected with *lp*11w and *lp*11w/Δ55K, we have observed efficient proteolytic processing of EGFR (Fig. 3). Since both viruses possess intact early E3 region, it is possible that the E3-RID protein may additionally target EGFR. Thus, the presence of the E3 region appears to be an asset that makes these vectors particularly useful for virotherapy of HNSCC. It should

be noted that most of the HAdV5 oncolytic vectors currently used worldwide are based on a parental HAdV5 mutant that contains a large deletion in the E3 region that includes the RID-coding region. In addition to E3, the E1A region may also transcriptionally down-regulate the expression of EGFR [42, 43]. Thus, the apoptotic activity and the ability to down-regulate the EGFR make these vectors as desirable agents for virotherapy of HNSCCs. The hamster pouch transplantation system and cell lines that we have developed should be useful in studying various chemotherapeutic agents in combination therapy with the apoptotic vectors studied here. Since the hamster pouches are immune privileged sites, it may also be possible to directly investigate the tumor growth inhibitory activities of the viral vectors against HNSCC under different immunomodulatory conditions.

Acknowledgments

This work was supported by research grants CA-33616 and CA-84941 from the National Cancer Institute and by a grant from the Lottie Caroline Hardy Charitable Trust. We thank W.S.M. Wold and Karoly Toth for their comments on the manuscript. We thank Jenni Franey and Anna Cline for their help with animal work.

References

1. Ries, L.; Young, J.; Keel, G.; Eisner, M.; Lin, Y.; Horner, M. SEER survival monograph: cancer survival among adults:SEER program 1998-2001, Patient and tumor characteristics. National Cancer Institute; Bethesda, MD: 2007. SEER Program; NIH Pub. No. 07-6215 2007
2. Huang SM, Bock JM, Harari PM. Epidermal growth factor receptor blockade with C225 modulates proliferation, apoptosis, and radiosensitivity in squamous cell carcinomas of the head and neck. Cancer Res. 1999; 59(8):1935–40. [PubMed: 10213503]
3. Bonner JA, Harari PM, Giralt J, Azarnia N, Shin DM, Cohen RB, et al. Radiotherapy plus cetuximab for squamous-cell carcinoma of the head and neck. N Engl J Med. 2006; 354(6):567–78. [PubMed: 16467544]
4. Baselga J, Schoffski P, Rojo F, Dumez H, Ramos FJ, Macarulla T, et al. A phase I pharmacokinetic (PK) and molecular pharmacodynamic (PD) study of the combination of two anti-EGFR therapies, the monoclonal antibody (MAb) cetuximab (C) and the tyrosine kinase inhibitor (TKI) gefitinib (G), in patients (pts) with advanced colorectal (CRC), head and neck (HNC) and non-small cell lung cancer (NSCLC). Journal of Clinical Oncology. 2006; 24(18):122s–122s.
5. Kalyankrishna S, Grandis JR. Epidermal growth factor receptor biology in head and neck cancer. J Clin Oncol. 2006; 24(17):2666–72. [PubMed: 16763281]
6. Reuter CW, Morgan MA, Eckardt A. Targeting EGF-receptor-signalling in squamous cell carcinomas of the head and neck. Br J Cancer. 2007; 96(3):408–16. [PubMed: 17224925]
7. Sharma H, Sen S, Lo Muzio L, Mariggio A, Singh N. Antisense-mediated downregulation of anti-apoptotic proteins induces apoptosis and sensitizes head and neck squamous cell carcinoma cells to chemotherapy. Cancer Biol Ther. 2005; 4(7):720–7. [PubMed: 15917659]
8. Bauer JA, Trask DK, Kumar B, Los G, Castro J, Lee JS, et al. Reversal of cisplatin resistance with a BH3 mimetic, (−)-gossypol, in head and neck cancer cells: role of wild-type p53 and Bcl-xL. Mol Cancer Ther. 2005; 4(7):1096–104. [PubMed: 16020667]
9. Vijayalingam S, Subramanian T, Ryerse J, Varvares M, Chinnadurai G. Down-regulation of multiple cell survival proteins in head and neck cancer cells by an apoptogenic mutant of adenovirus type 5. Virology. 2009; 392(1):62–72. [PubMed: 19631957]
10. Blackford AN, Grand RJ. Adenovirus E1B 55-kilodalton protein: multiple roles in viral infection and cell transformation. J Virol. 2009; 83(9):4000–12. [PubMed: 19211739]
11. O'Shea CC, Johnson L, Bagus B, Choi S, Nicholas C, Shen A, et al. Late viral RNA export, rather than p53 inactivation, determines ONYX-015 tumor selectivity. Cancer Cell. 2004; 6(6):611–23. [PubMed: 15607965]

12. Khuri FR, Nemunaitis J, Ganly I, Arseneau J, Tannock IF, Romel L, et al. a controlled trial of intratumoral ONYX-015, a selectively-replicating adenovirus, in combination with cisplatin and 5-fluorouracil in patients with recurrent head and neck cancer. Nat Med. 2000; 6(8):879–85. [PubMed: 10932224]
13. Chia MC, Shi W, Li JH, Sanchez O, Strathdee CA, Huang D, et al. A conditionally replicating adenovirus for nasopharyngeal carcinoma gene therapy. Mol Ther. 2004; 9(6):804–17. [PubMed: 15194047]
14. Toivonen R, Suominen E, Grenman R, Savontaus M. Retargeting improves the efficacy of a telomerase-dependent oncolytic adenovirus for head and neck cancer. Oncol Rep. 2009; 21(1): 165–71. [PubMed: 19082458]
15. Blackwell JL, Miller CR, Douglas JT, Li H, Reynolds PN, Carroll WR, et al. Retargeting to EGFR enhances adenovirus infection efficiency of squamous cell carcinoma. Arch Otolaryngol Head Neck Surg. 1999; 125(8):856–63. [PubMed: 10448731]
16. Boyle JO, Hakim J, Koch W, van der Riet P, Hruban RH, Roa RA, et al. The incidence of p53 mutations increases with progression of head and neck cancer. Cancer Res. 1993; 53(19):4477–80. [PubMed: 8402617]
17. Pan JJ, Zhang SW, Chen CB, Xiao SW, Sun Y, Liu CQ, et al. Effect of recombinant adenovirusp53 combined with radiotherapy on long-term prognosis of advanced nasopharyngeal carcinoma. J Clin Oncol. 2009; 27(5):799–804. [PubMed: 19103729]
18. Nemunaitis J. Head and neck cancer: response to p53-based therapeutics. Head Neck. 2011; 33(1): 131–4. [PubMed: 20222046]
19. Peng Z. Current status of gendicine in China: recombinant human Ad-p53 agent for treatment of cancers. Hum Gene Ther. 2005; 16(9):1016–27. [PubMed: 16149900]
20. Thomas MA, Spencer JF, La Regina MC, Dhar D, Tollefson AE, Toth K, et al. Syrian hamster as a permissive immunocompetent animal model for the study of oncolytic adenovirus vectors. Cancer Res. 2006; 66(3):1270–6. [PubMed: 16452178]
21. Bortolanza S, Alzuguren P, Bunuales M, Qian C, Prieto J, Hernandez-Alcoceba R. Human adenovirus replicates in immunocompetent models of pancreatic cancer in Syrian hamsters. Hum Gene Ther. 2007; 18(8):681–90. [PubMed: 17658991]
22. Hasegawa N, Abei M, Yokoyama KK, Fukuda K, Seo E, Kawashima R, et al. Cyclophosphamide enhances antitumor efficacy of oncolytic adenovirus expressing uracil phosphoribosyltransferase (UPRT) in immunocompetent Syrian hamsters. Int J Cancer. 2013; 133(6):1479–88. [PubMed: 23444104]
23. Spencer JF, Sagartz JE, Wold WS, Toth K. New pancreatic carcinoma model for studying oncolytic adenoviruses in the permissive Syrian hamster. Cancer Gene Ther. 2009; 16(12):912–22. [PubMed: 19478829]
24. Adams J, Heintz P, Gross N, Andersen P, Everts E, Wax M, et al. Acid/pepsin promotion of carcinogenesis in the hamster cheek pouch. Arch Otolaryngol Head Neck Surg. 2000; 126(3):405–9. [PubMed: 10722017]
25. Manoharan S, Balakrishnan S, Menon VP, Alias LM, Reena AR. Chemopreventive efficacy of curcumin and piperine during 7,12-dimethylbenz[a]anthracene-induced hamster buccal pouch carcinogenesis. Singapore Med J. 2009; 50(2):139–46. [PubMed: 19296028]
26. Min BM, Kim K, Cherrick HM, Park NH. Three cell lines from hamster buccal pouch tumors induced by topical 7,12-dimethylbenz(a)anthracene, alone or in conjunction with herpes simplex virus inoculation. In Vitro Cell Dev Biol. 1991; 27A(2):128–36. [PubMed: 1708371]
27. Subramanian T, Vijayalingam S, Chinnadurai G. Genetic identification of adenovirus type 5 genes that influence viral spread. J Virol. 2006; 80(4):2000–12. [PubMed: 16439556]
28. Gonzalez R, Huang W, Finnen R, Bragg C, Flint SJ. Adenovirus E1B 55-kilodalton protein is required for both regulation of mRNA export and efficient entry into the late phase of infection in normal human fibroblasts. J Virol. 2006; 80(2):964–74. [PubMed: 16378998]
29. Slaga TJ, Gimenez-Conti IB. An animal model for oral cancer. J Natl Cancer Inst Monogr. 1992; (13):55–60. [PubMed: 1382504]

30. Wold WS, Toth K. Chapter three--Syrian hamster as an animal model to study oncolytic adenoviruses and to evaluate the efficacy of antiviral compounds. Adv Cancer Res. 2012; 115:69–92. [PubMed: 23021242]
31. Bongers V, Braakhuis BJ, Snow GB. Circulating fragments of cytokeratin 19 in patients with head and neck squamous cell carcinoma. Clin Otolaryngol Allied Sci. 1995; 20(5):479–82. [PubMed: 8582085]
32. Xu XC, Lee JS, Lippman SM, Ro JY, Hong WK, Lotan R. Increased expression of cytokeratins CK8 and CK19 is associated with head and neck carcinogenesis. Cancer Epidemiol Biomarkers Prev. 1995; 4(8):871–6. [PubMed: 8634660]
33. Becker MT, Shores CG, Yu KK, Yarbrough WG. Molecular assay to detect metastatic head and neck squamous cell carcinoma. Arch Otolaryngol Head Neck Surg. 2004; 130(1):21–7. [PubMed: 14732763]
34. Chinnadurai G. Control of apoptosis by human adenovirus genes. Seminars in Virology. 1998; 8(5):399–408.
35. Cuconati A, White E. Viral homologs of BCL-2: role of apoptosis in the regulation of virus infection. Genes Dev. 2002; 16(19):2465–78. [PubMed: 12368257]
36. Thomas MA, Spencer JF, Toth K, Sagartz JE, Phillips NJ, Wold WS. Immunosuppression enhances oncolytic adenovirus replication and antitumor efficacy in the Syrian hamster model. Mol Ther. 2008; 16(10):1665–73. [PubMed: 18665155]
37. Young BA, Spencer JF, Ying B, Tollefson AE, Toth K, Wold WS. The role of cyclophosphamide in enhancing antitumor efficacy of an adenovirus oncolytic vector in subcutaneous Syrian hamster tumors. Cancer Gene Ther. 2013; 20(9):521–30. [PubMed: 23928731]
38. Rowinsky EK. The erbB family: targets for therapeutic development against cancer and therapeutic strategies using monoclonal antibodies and tyrosine kinase inhibitors. Annu Rev Med. 2004; 55:433–57. [PubMed: 14746530]
39. Herbst RS, Fukuoka M, Baselga J. Gefitinib--a novel targeted approach to treating cancer. Nat Rev Cancer. 2004; 4(12):956–65. [PubMed: 15573117]
40. Carlin CR, Tollefson AE, Brady HA, Hoffman BL, Wold WS. Epidermal growth factor receptor is down-regulated by a 10,400 MW protein encoded by the E3 region of adenovirus. Cell. 1989; 57(1):135–44. [PubMed: 2522818]
41. Tollefson AE, Stewart AR, Yei SP, Saha SK, Wold WS. The 10,400- and 14,500-dalton proteins encoded by region E3 of adenovirus form a complex and function together to down-regulate the epidermal growth factor receptor. J Virol. 1991; 65(6):3095–105. [PubMed: 1851870]
42. Flinterman MB, Mymryk JS, Klanrit P, Yousef AF, Lowe SW, Caldas C, et al. p400 function is required for the adenovirus E1A-mediated suppression of EGFR and tumour cell killing. Oncogene. 2007; 26(48):6863–74. [PubMed: 17486071]
43. Flinterman M, Gaken J, Farzaneh F, Tavassoli M. E1A-mediated suppression of EGFR expression and induction of apoptosis in head and neck squamous carcinoma cell lines. Oncogene. 2003; 22(13):1965–77. [PubMed: 12673202]

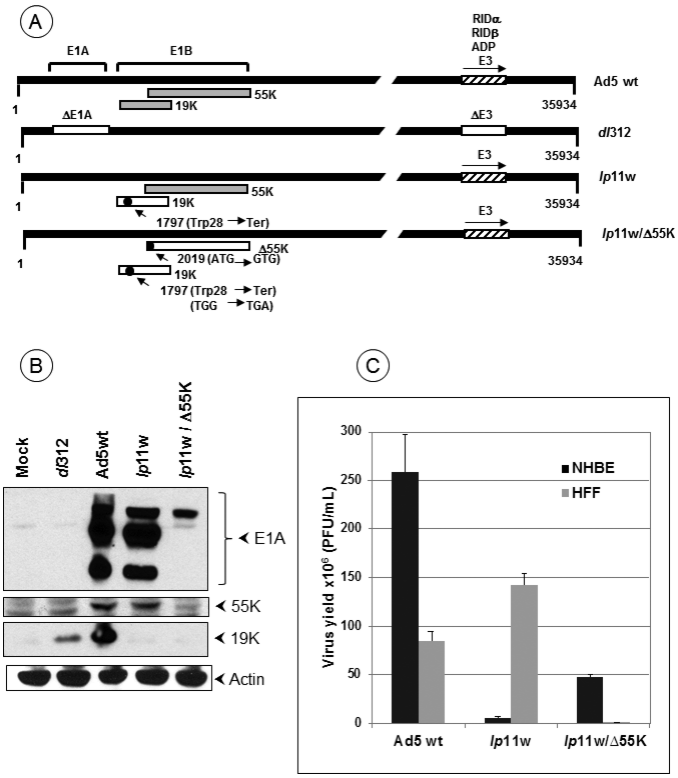

Figure 1. HAdV5 mutants and replication in normal cells

(A). Diagrammatic illustration of HAdV5 mutants. The top panel shows the proteins expressed from early regions E1B and E3. Mutants *lp*11w and *lp*11w/Δ55K express wt E1A and E3 regions while the control mutant *dl*312 contain deletions in these regions. The mutations within the E1B region are indicated. (B). Expression of E1A and E1B proteins by HAdV5 mutants. (C). Replication of HAdV5 mutants in normal human epithelial (NHBE) and fibroblast (HFF) cells. The virus yield from infected NHBE and HFF cells were determined by plaque assay on 293 cells.

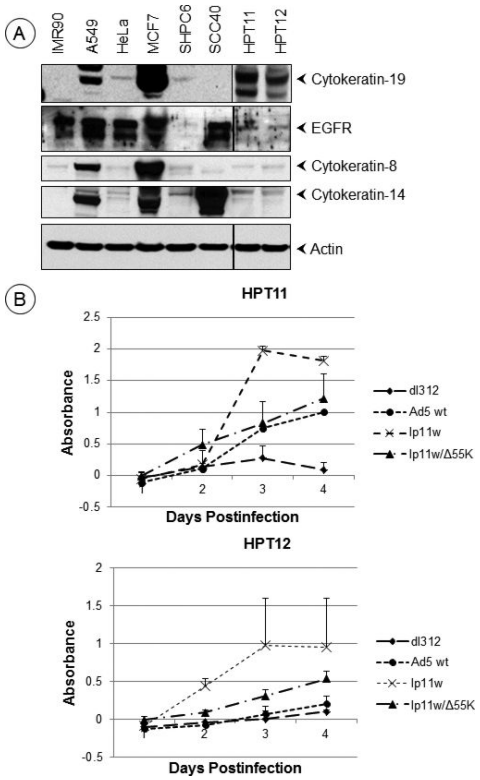

Figure 2. Cytolytic activity of E1B mutants in hamster cell lines

(A). Expression of cytokeratins in hamster cell lines. The western blots were probed with antibodies against human cytokeratins 8, 14 and 19, EGFR and actin. (B). Cytolytic activity of HAdV5 mutants. The hamster cell lines HPT11 and 12 were infected with HAdV5 wt or mutants at 500 PFU/cell and the cytolytic activity was determined by the lactate dehydrogenase (LDH) release assay using CytoTox 96 Non-Radioactive cytotoxicity assay kit (Promega).

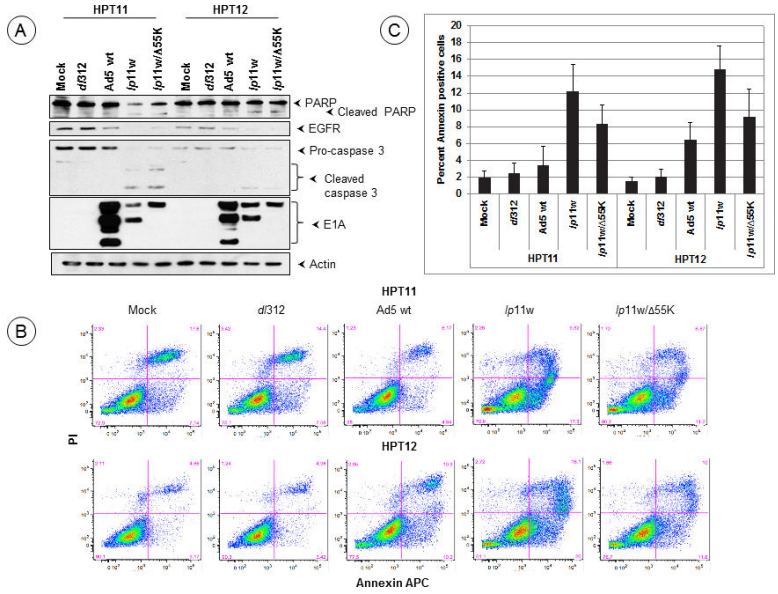

Figure 3. Apoptotic activity of HAdV5 mutants in hamster cells

(A). Effect of HAdV5 mutants on caspase activation. HPT11 and 12 cells were infected with indicated mutants at 400 PFU/cell and proteolytic processing of pro-caspase 3, EGFR and PARP were determined by western blot analysis 24 hr after infection. (B). HPT11 and 12 cells were infected 400 PFU/cell and the annexin V-staining patterns were determined by FACS analysis. A representative analysis is shown in B. (C). Averages of annexin V-positive cells were shown as an indication of apoptotic cell death. The experiment was repeated at least three times independently and the data are means ±SD. Statistical differences were assessed using one-way ANOVA followed by a Newman-Keuls Multiple Comparision Test, where appropriate, using GraphPad Prism 5 software. *P*-Value was determined by comparing mock, *dl*312 and Ad5 wt vs *lp*11w and mock, *dl*312 and Ad5 wt vs *lp*11w/Δ55K in both HPT11 and HPT12 cell lines. Statistical significance was accepted at a value of $*P<0.05$ and $**P<0.001$.

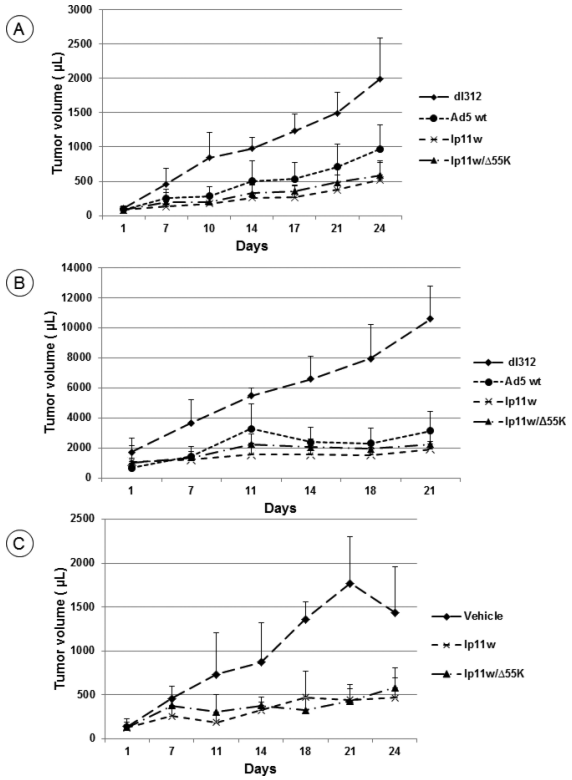

Figure 4. Oncolytic activity of HAdV5 vectors against subcutaneous tumors induced by hamster pouch tumor cell lines

(A). Athymic mice were subcutaneously transplanted with HPT12 cells and the tumors were injected with indicated HAdV5 mutants. At 24 days post treatment, the tumor measurements indicated significant reduction in tumor growth by the administration of HAdv5 wt, *lp*11w or *lp*11w/Δ55K compared to the administration of *dl*312 (p=0.0072, 0.0018, and 0.0072 respectively). Comparison between tumors treated with *lp*11w and tumors treated with HAdV5 wt indicated significant suppression by *lp*11w (p=0.0198). Similarly, the growth of tumors treated with *lp*11w/Δ55K was significantly suppressed compared to HAdV5 wt treated tumors (p=0.0044). n=5 mice.

(B). The hamster tumor cell line HPT12 was subcutaneously transplanted at the hamster hind flanks and the tumors were treated with *lp*11w or *lp*11w/Δ55K or *dl*312. The tumor measurements at 21 days post treatment indicated that *lp*11w and *lp*11w/Δ55K significantly suppressed tumor growth compared to treatment with *dl*312 (p=0.0014 and 0.0010, respectively). At 18 days, the tumors treated with *lp*11w or *lp*11w/Δ55K viruses were significantly suppressed compared to those treated with *dl*312 (p=0.0044 and 0.0049, respectively). n=4 hamsters

(C). The hamsters were subcutaneously transplanted with HPT11 cells at the hind flanks and the tumors were treated with *lp*11w, *lp*11w/Δ55K or vehicle. At 24 days post treatment, *lp*11w and *lp*11wΔ55K significantly suppressed the tumor growth compared to the vehicle (p=0.0001 and 0.001 respectively). At 21 days, the significance levels were p=0.0001 and 0.0001, respectively. At 18 days, the significance levels were p=0.001 and 0.0001, respectively. n=4 hamsters

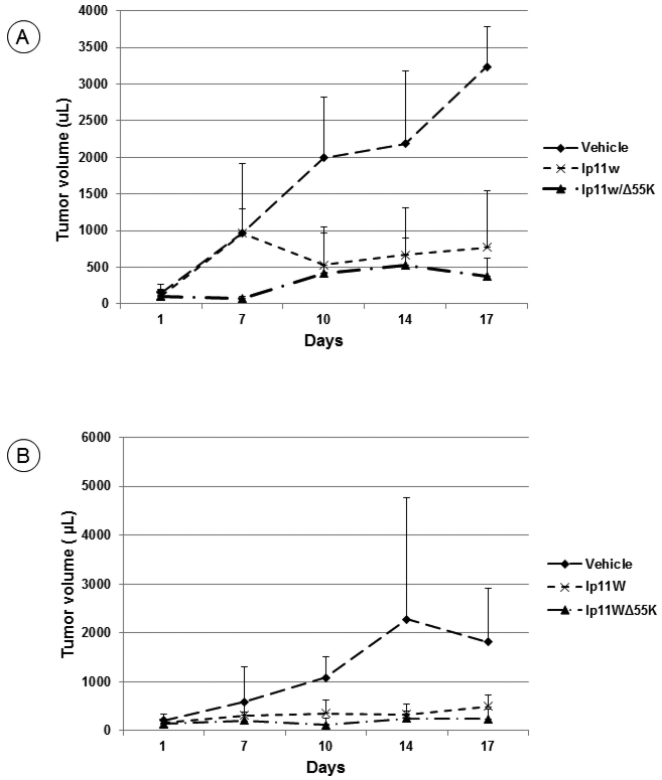

Figure 5. Oncolytic activity of HAdV5 vectors against orthotopic tumors induced by the hamster cheek pouch tumor cell lines

(A). Orthotopic tumors in the hamster cheek pouches were generated by transplantation of HPT12 cells and the tumors were administered with *lp*11w or *lp*11w/Δ55K or the vehicle. At 17 days, both viruses significantly suppressed the tumor growth compared to the vehicle (p=0.001 and 0.0005, respectively). At 14 days, the levels of significance were p=0.021 and 0.0184, respectively) and at 10 days the significance levels were p=0.030 and 0.0252, respectively. n=4 hamsters.

(B). Hamster cheek pouch tumors were generated by transplantation of HPT11 cells and the tumors were administered with *lp*11w or *lp*11w/Δ55K or the vehicle. At 17 days, the administration of *lp*11w or *lp*11w/Δ55K viruses significantly suppressed the tumor growth compared to the vehicle control (p=0.021 and 0.030, respectively). At 10 days the significance levels were p=0.033 and 0.0153, respectively. N=4 hamsters.

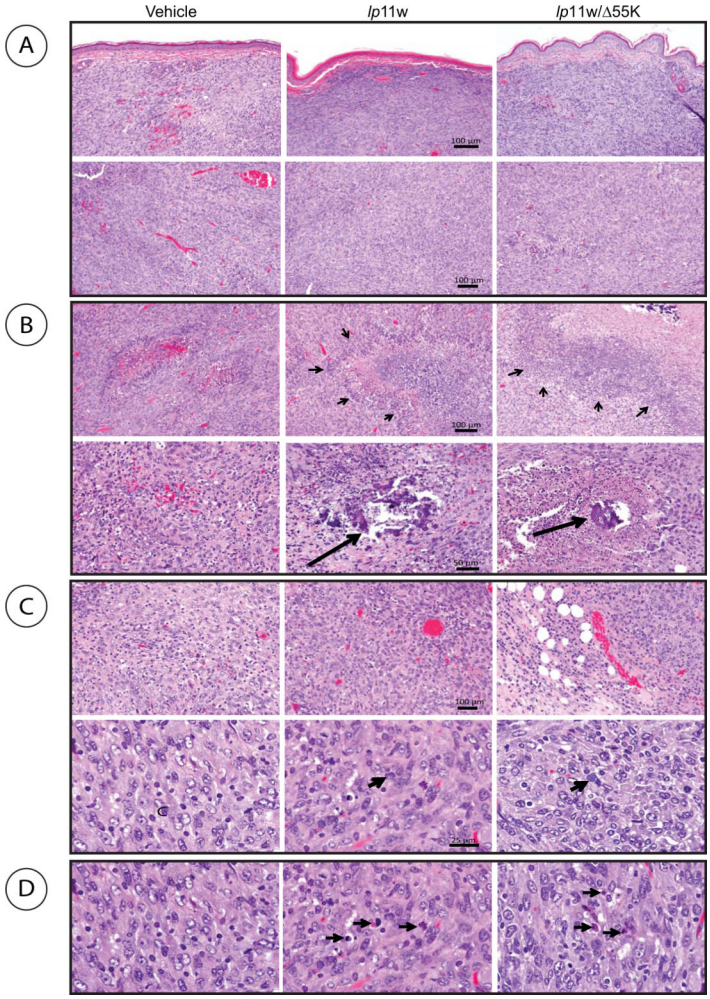

Fig. 6. Histology of hamster cheek pouch tumors treated with HAdV5 vectors

Tumor sections were stained with hematoxylin-eosin and photographed. The size bars indicate 100 μm (top three panels), 50 μm (fourth panel), 100 μm (fifth panel) and 25 μm (sixth panel). (A). Vascularity of treated tumors. (B). Necrosis and calcification in treated tumors. (C). Presence of cells like plasma cells. (D). Presence of apoptotic features.

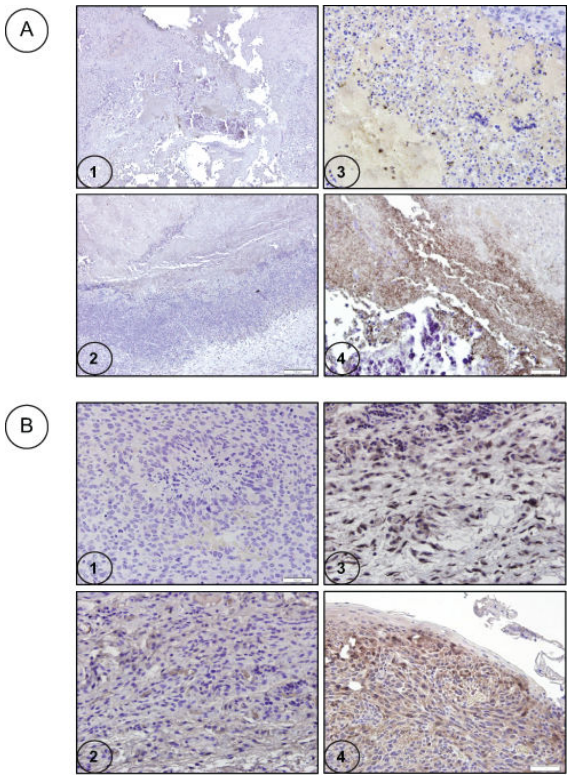

Figure 7. Immunocytochemistry of virus-treated pouch tumors

Immunocytochemistry analysis was performed with tumor sections using anti-fiber antibody (A) or caspase-3 antibody (B). 1. Representative vehicle-treated tumor section 2. Section of tumor-treated with *lp*11w/Δ55K and stained with the isotype (mouse IgG) antibody control 3. Section of tumor treated with *lp*11w and stained with the anti-fiber or caspase-3 antibody 4. Section of tumor-treated with *lp*11w/Δ55K and stained with the anti-fiber or caspase-3 antibody. The size bars indicate 200 μm (A1 and 2) and 50 μm (A3 and 4 and B1-4).

Table 1

Anti-HAdv5 antibody in sera from tumor bearing hamsters treated with adenoviral vectors

Serum (HPT11)	Serological test	Serum (HPT 12)	Serological test
Subcutaneous tumors			
Vehicle	-	Vehicle	40
*Ip*11w	720	*Ip*11w	180
*Ip*11w/Δ55K	960	*Ip*11w/Δ55K	240
		Ad5 wt	1280
Pouch tumors			
Vehicle	-	Vehicle	-
*Ip*11w	480	*Ip*11w	1440
*Ip*11w/Δ55K	640	*Ip*11w/Δ55K	640

Neutralizing antibody titers are expressed as the highest reciprocal serum dilutions. Average antibody titers from two animals from each group are presented. Hyper immunized serum raised against HAdV5 wt virus from hamster was used for positive control.